



Algorithm Theoretical Basis Document (ATBD) – ANNEX E for IASI CO₂ (v10.1) and CH₄ (v10.2) and AIRS CO₂ mid-tropospheric products

C3S2_312a_Lot2_DLR – Atmosphere

Issued by: C. Crevoisier, LMD/CNRS, France

Date: 01/02/2024

Ref: C3S2_312a_Lot2_D-WP1_ATBD-2023-GHG_ANNEX-D_v7.1b

Official reference number service contract: 2021/C3S2_312a_Lot2_DLR/SC1





This document has been produced in the context of the Copernicus Climate Change Service (C3S). The activities leading to these results have been contracted by the European Centre for Medium-Range Weather Forecasts, operator of C3S on behalf on the European Union (Contribution Agreement signed on 22/07/2021). All information in this document is provided “as is” and no guarantee of warranty is given that the information is fit for any particular purpose. The users thereof use the information at their sole risk and liability. For the avoidance of all doubt, the European Commission and the European Centre for Medium-Range Weather Forecasts have no liability in respect of this document, which is merely representing the author’s view.



Contributors

**INSTITUTE OF ENVIRONMENTAL PHYSICS (IUP),
UNIVERSITY OF BREMEN, BREMEN, GERMANY
(IUP)**

M. Buchwitz

**CENTRE NATIONAL DE LA RECHERCHE SCIENTIFIQUE (CNRS),
LABORATOIRE DE METEOROLOGIE DYNAMIQUE (LMD),
PALAISEAU, FRANCE
(LMD/CNRS)**

C. Crevoisier

N. Meilhac



History of modifications

Version	Date	Description of modification	Chapters / Sections
1.1	20-October-2017	New document for data set CDR1 (until 2016)	All
2.0	4-October-2018	Update for CDR2 (until 2017)	All
3.0	12-August-2019	Update for CDR3 (until 2018) with additional information on Metop-A and Metop-C processing	All (especially Sects. 2.1 and 3.1)
3.1	03-November-2019	Update after review by Assimila	All
4.0 beta	18-August-2020	Update for CDR4 with new version for all IASI products	All
4.0	17-September-2020	Correction of typos after review	Sections 2.1.2 and 3.1.4.2
5.0	18-February-2021	Update for CDR5 (until 2020)	All
6.0 Draft	18-February-2022	Update for CDR6 (until 2021)	All
6.0	4-August-2022	Update for CDR6 (until 2021)	All
6.1	25-November-2022	Update after review (use of new template, various mostly minor improvements at several places)	All
6.2	31-January-2023	Minor improvements at various places taking into account feedback from 2 nd review	All
7.0 (Draft 1)	23-February-2023	Initial draft for data set CDR7 ("Draft-ATBD")	All
7.0 (Draft 2)	27-April-2023	Updates taking into account feedback from independent review	All
7.0 (Draft 4)	3-August-2023	Improved Draft after review	All
7.0	28-August-2023	Update for data set CDR7	All
7.1	13-September-2023	Minor improvements	All
7.1b	1-February-2024	Flow diagram (Fig. 3) added; several minor improvements	All



List of datasets covered by this document

Deliverable ID	Product title	Product type (CDR, ICDR)	Version number	Delivery date
WP2-FDDP-GHG-v2	CO2_IASA_NLIS	CDR 7	10.1	31-Aug-2023
	CH4_IASA_NLIS		10.2	
	CO2_IASB_NLIS		10.1	
	CH4_IASB_NLIS		10.2	
	CO2_IASC_NLIS		10.1	
	CH4_IASC_NLIS		10.2	

Related documents

Reference ID	Document
D1	<p>Main ATBD:</p> <p>Buchwitz, M., et al., Algorithm Theoretical Basis Document (ATBD) – Main document for Greenhouse Gas (GHG: CO₂ & CH₄) data set CDR 7 (2003-2022), project C3S2_312a_Lot2_DLR – Atmosphere, v7.1, 2023.</p> <p><i>(this document is an ANNEX to the Main ATBD)</i></p>



Acronyms

Acronym	Definition
AIRS	Atmospheric Infrared Sounder
AMSU	Advanced Microwave Sounding Unit
ATBD	Algorithm Theoretical Basis Document
BESD	Bremen optimal ESTimation DOAS
CAR	Climate Assessment Report
C3S	Copernicus Climate Change Service
CCDAS	Carbon Cycle Data Assimilation System
CCI	Climate Change Initiative
CDR	Climate Data Record
CDS	(Copernicus) Climate Data Store
CMUG	Climate Modelling User Group (of ESA's CCI)
CRG	Climate Research Group
D/B	Data base
DOAS	Differential Optical Absorption Spectroscopy
EC	European Commission
ECMWF	European Centre for Medium Range Weather Forecasting
ECV	Essential Climate Variable
EMMA	Ensemble Median Algorithm
ENVISAT	Environmental Satellite (of ESA)
EO	Earth Observation
ESA	European Space Agency
EU	European Union
EUMETSAT	European Organisation for the Exploitation of Meteorological Satellites
FCDR	Fundamental Climate Data Record
FoM	Figure of Merit
FP	Full Physics retrieval method
FTIR	Fourier Transform InfraRed
FTS	Fourier Transform Spectrometer
GCOS	Global Climate Observing System
GEO	Group on Earth Observation
GEOSS	Global Earth Observation System of Systems
GHG	GreenHouse Gas
GOS	GOSAT
GO2	GOSAT-2
GOME	Global Ozone Monitoring Experiment
GMES	Global Monitoring for Environment and Security



GOSAT	Greenhouse Gases Observing Satellite
GOSAT-2	Greenhouse Gases Observing Satellite 2
IASI	Infrared Atmospheric Sounding Interferometer
IMAP-DOAS (or IMAP)	Iterative Maximum A posteriori DOAS
IPCC	International Panel in Climate Change
IUP	Institute of Environmental Physics (IUP) of the University of Bremen, Germany
JAXA	Japan Aerospace Exploration Agency
JCGM	Joint Committee for Guides in Metrology
L1	Level 1
L2	Level 2
L3	Level 3
L4	Level 4
LMD	Laboratoire de Météorologie Dynamique
MACC	Monitoring Atmospheric Composition and Climate, EU GMES project
NA	Not applicable
NASA	National Aeronautics and Space Administration
NetCDF	Network Common Data Format
NDACC	Network for the Detection of Atmospheric Composition Change
NIES	National Institute for Environmental Studies
NIR	Near Infra-Red
NLIS	LMD/CNRS <i>neuronal</i> network mid/upper tropospheric CO ₂ and CH ₄ retrieval algorithm
NOAA	National Oceanic and Atmospheric Administration
Obs4MIPs	Observations for Climate Model Intercomparisons
OCFP	OCO-2 Full Physics (FP) algorithm (used by Univ. Leicester)
OCO	Orbiting Carbon Observatory
OCPR	OCO-2 Proxy (PR) algorithm (used by Univ. Leicester)
OE	Optimal Estimation
PBL	Planetary Boundary Layer
ppb	Parts per billion
ppm	Parts per million
PQAD	Product Quality Assurance Document
PQAR	Product Quality Assessment Report
PR	(light path) PROxy retrieval method
PVIR	Product Validation and Intercomparison Report
QA	Quality Assurance
QC	Quality Control
RemoTeC	Retrieval algorithm developed by SRON
REQ	Requirement
RMS	Root-Mean-Square



RTM	Radiative transfer model
SCIAMACHY	SCanning Imaging Absorption spectroMeter for Atmospheric Chartography
SCIATRAN	SCIAMACHY radiative transfer model
SRON	SRON Netherlands Institute for Space Research
SRFP	SRON's Full Physics (FP) algorithm (also referred to a RemoTeC FP)
SRPR	SRON's Proxy (PR) algorithm (also referred to a RemoTeC PR)
SWIR	Short Wave InfraRed
TANSO	Thermal And Near infrared Sensor for carbon Observation
TANSO-FTS	Fourier Transform Spectrometer on GOSAT
TANSO-FTS-2	Fourier Transform Spectrometer on GOSAT-2
TBC	To be confirmed
TBD	To be defined / to be determined
TCCON	Total Carbon Column Observing Network
TIR	Thermal InfraRed
TR	Target Requirements
TRD	Target Requirements Document
WFM-DOAS (or WFMD)	Weighting Function Modified DOAS
UoL	University of Leicester, United Kingdom
URD	User Requirements Document
WMO	World Meteorological Organization
Y2Y	Year-to-year (bias variability)



General definitions

Essential climate variable (ECV)

An ECV is a physical, chemical, or biological variable or a group of linked variables that critically contributes to the characterization of Earth's climate.

Climate data record (CDR)

The US National Research Council (NRC) defines a CDR as a time series of measurements of sufficient length, consistency, and continuity to determine climate variability and change.

Fundamental climate data record (FCDR)

A fundamental climate data record (FCDR) is a CDR of calibrated and quality-controlled data designed to allow the generation of homogeneous products that are accurate and stable enough for climate monitoring.

Thematic climate data record (TCDR)

A thematic climate data record (TCDR) is a long time series of an essential climate variable (ECV).

Intermediate climate data record (ICDR)

An intermediate climate data record (ICDR) is a TCDR which undergoes regular and consistent updates, for example because it is being generated by a satellite sensor in operation.

Satellite data processing levels

The NASA Earth Observing System (EOS) distinguishes six processing levels of satellite data, ranging from Level 0 (L0) to Level 4 (L4) as follows.

- L0 Unprocessed instrument data
- L1A Unprocessed instrument data alongside ancillary information
- L1B Data processed to sensor units (geo-located calibrated spectral radiance and solar irradiance)
- L2 Derived geophysical variables (e.g., XCO₂) over one orbit
- L3 Geophysical variables averaged in time and mapped on a global longitude/latitude horizontal grid
- L4 Model output derived by assimilation of observations, or variables derived from multiple measurements (or both)



Table of Contents

History of modifications	4
List of datasets covered by this document	5
Related documents	5
Acronyms	6
General definitions	9
Scope of document	12
Executive summary	13
1. Instruments	14
1.1.1 The IASI instrument onboard the Metop satellites	14
1.1.2 The AMSU instrument onboard the Metop satellites	15
1.1.3 The AIRS and AMSU instruments onboard the Aqua satellite	15
2. Input and auxiliary data	17
2.1 Level 1 data	17
2.2 Other data	17
2.2.1 The TIGR database	17
2.2.2 The ARSA database	17
3. Algorithms	18
3.1 Algorithm for IASI mid-tropospheric CO₂ and CH₄ retrieval	18
3.1.1 General description	18
3.1.2 Forward model and spectroscopic database	19
3.1.3 Channel selection	19
3.1.4 Neural architecture	21
3.1.5 Training of the networks	23
3.1.6 Application to observations	26
3.1.7 Vertical characterization of the retrieval	30
3.2 Algorithm for AIRS mid-tropospheric CO₂ retrieval	33
3.2.1 General description	33
3.2.2 Forward model and spectroscopic database	33
3.2.3 Channel selection	34
3.2.4 Neural architecture	34
3.2.5 Training of the networks	35
3.2.6 Application to observations	36
3.2.7 Vertical characterization of the retrieval	38



4. Output data	39
References	43



Scope of document

This document is an Algorithm Theoretical Basis Document (ATBD) for the Copernicus Climate Change Service (C3S, <https://climate.copernicus.eu/>) greenhouse gas (GHG) component as covered by project C3S3_312a_Lot2.

Within this project satellite-derived atmospheric carbon dioxide (CO₂) and methane (CH₄) Essential Climate Variable (ECV) data products are generated and delivered to ECMWF for inclusion into the Copernicus Climate Data Store (CDS) from which users can access these data products and the corresponding documentation.

The satellite-derived GHG data products are:

- Column-averaged dry-air mixing ratios (mole fractions) of CO₂ and CH₄, denoted XCO₂ (in parts per million, ppm) and XCH₄ (in parts per billion, ppb), respectively.
- Mid/upper tropospheric mixing ratios of CO₂ (in ppm) and CH₄ (in ppb).

This document describes the retrieval algorithms (CNRS-LMD *Non Linear Inference Scheme* -NLIS) to generate the C3S products CO₂_IASA_NLIS, CH₄_IASA_NLIS, CO₂_IASB_NLIS, CH₄_IASB_NLIS, CO₂_IASC_NLIS and CH₄_IASC_NLIS.

These products are mid-tropospheric CO₂ and CH₄ Level 2 products as retrieved from the Infrared Atmospheric Sounding Interferometer (IASI) sensors on Metop-A, Metop-B and Metop-C European platforms using algorithms developed at CNRS-LMD, France.

The NLIS algorithm is also used to retrieve mid-tropospheric CO₂ from AIRS (product CO₂_AIR_NLIS) and a description of NLIS as applied to AIRS is also given in this document.



Executive summary

This document describes the retrieval algorithms developed at CNRS-LMD to retrieve mid-tropospheric column of CO₂ and CH₄ from the IASI and AMSU instruments flying onboard the European Metop satellites. It details the various input data required for retrievals, the physical theory, and the mathematical background underlying retrieval assumptions, and also outlines the retrieval implementation and the limitations of the approach used.

The Non Linear Inference Scheme (NLIS) algorithms are based on the non-linear regression inverse radiative transfer model using Multi-Layer Perceptrons (Crevoisier et al., 2009a, 2009b), that was first designed to retrieve CO₂ from the first generation TOVS instruments flying onboard the NOAA polar platforms (Chédin et al., 2003). The input data are radiances measured by IASI and AMSU instruments onboard Metop-A (2007-2021), Metop-B (since 2013) and Metop-C (since 2019) space platforms. IASI and AMSU instruments are vertical sounders measuring in the thermal infrared and microwave spectral domains, respectively. Auxiliary data are also used to provide additional information on the atmosphere. The output data are mid-tropospheric columns of CO₂ and CH₄, to which are associated vertical weighting functions that give information on the sensitivity of IASI to variations of the gases along the atmospheric column.

Throughout the lifetime of the missions, changes have happened at instrument level (spectral changes, noise increase) in 2015, 2017, 2019 and 2021. They had an impact on the retrievals themselves. Successive versions of the retrieval scheme have thus been designed to cope with these changes. They are detailed in the document.

Section 1 gives an overview of the data product including a description of the satellites. Section 2 introduces the various input data which enter into the retrieval algorithm. Sections 3 and 4 describe in detail the retrieval algorithm and its output, respectively.



1. Instruments

1.1.1 The IASI instrument onboard the Metop satellites

The Infrared Atmospheric Sounding Interferometer (IASI) is a high resolution Fourier Transform Spectrometer based on a Michelson Interferometer coupled to an integrated imaging system that measures infrared radiation emitted from the Earth (<https://iasi.cnes.fr/en/IASI/index.htm>). Developed by the Center National d'Etudes Spatiales (CNES) in collaboration with the European Organisation for the Exploitation of Meteorological Satellites (EUMETSAT), IASI was launched in October 2006 onboard the polar orbiting Meteorological Operational Platform (Metop-A), in September 2012 onboard Metop-B, and in October 2018 onboard Metop-C. Metop-A has been decommissioned in November 2022, after 15 years of nominal operation. The last data delivery happened on October 15th 2022. Starting in late August 2021, so-called end-of-life experiments were conducted by CNES and EUMETSAT, yielding a few days without data, as well as a full month (September 15th to October 15th 2022) with IASI operating in a narrow swath configuration (220 km instead of 2200 km) in order to provide oversampling along the orbits.

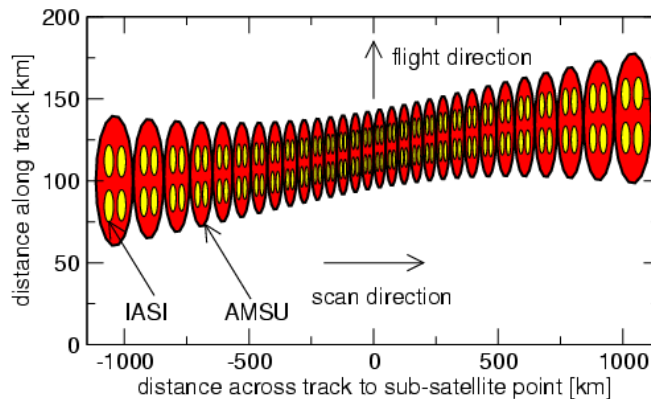
The comparison between the 3 IASI instruments at Level 1 shows that the three instruments agree at the level of 0.1 K or less for most of the spectrum.

IASI provides 8461 spectral samples, ranging from 645 cm⁻¹ to 2760 cm⁻¹ (15.5 μm and 3.6 μm), with a spectral sampling of 0.25 cm⁻¹, and a spectral resolution of 0.5 cm⁻¹. IASI is an across track scanning system, whose swath width is of 2200 km, allowing global coverage twice a day. The IFOV is sampled by 2×2 circular pixels whose ground resolution is 12 km at nadir at 9:30 am/pm local time.

The combined use of both Metop satellites, which are flying on the same orbit but with nearly half an orbit out of phase, yields a complete coverage of the Earth in one day. Combining Metop-A, -B and -C, the time series will cover about 20 years. In order to be useful for climate studies, it is mandatory that the time series derived from the 3 successive platforms are consistent in order to allow the study of trends and growth rates of several essential climate variables such as greenhouse gases.



Figure 1: IASI and AMSU scanning geometry IASI individual field of views are shown as yellow circles while AMSU individual field of views are shown as red circles (from IASI Level 1 Product Guide available at http://eodg.atm.ox.ac.uk/user/dudhia/iasi/documents/PDF_IASI_LEVEL_1_PROD_GUIDE.pdf).



1.1.2 The AMSU instrument onboard the Metop satellites

Also flying onboard Metop satellites is the AMSU-A (Advanced Microwave Sounding Unit) instrument, which is a 15-channel microwave radiometer, which measures scene radiances in 15 discrete frequency channels spanning 23–90 GHz. Thirty consecutive field of views of 48 km diameter at nadir are sampled, yielding a 2,074 km swath width. AMSU-A uses oxygen absorption bands/lines for atmospheric temperature sounding, while window channels provide information on surface temperature and emissivity.

As seen in Figure 1, scanning of both sounders is synchronized, with 4 IASI fields of view (FOV) (yellow lozenges) embedded in 1 AMSU FOV (red lozenge), allowing the same atmospheric situation to be simultaneously observed by both instruments.

On all Metop satellites, several AMSU channels have experienced behaviors outside of specifications. In particular, among the 3 AMSU channels 6, 7 and 8 that are particularly important for the retrieval procedure, only AMSU 6 channels are available for all Metop satellites for the whole time period covered by each satellite. For instance, for Metop-A, the AMSU 7 channel stopped operating in 2008 while AMSU 8 channels stopped operating in 2015. This has led to some changes in the retrieval procedure that are described below.

1.1.3 The AIRS and AMSU instruments onboard the Aqua satellite

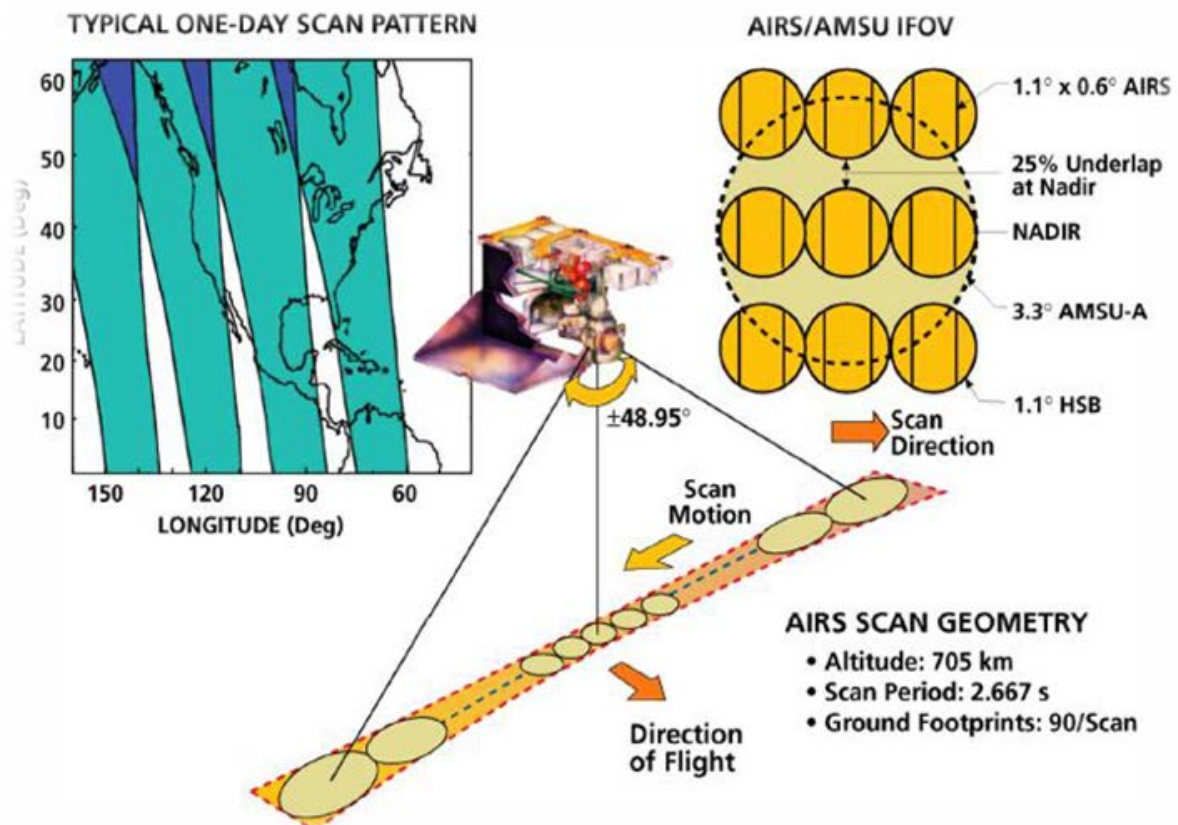
The Atmospheric Infrared Sounder (AIRS) is a polar orbiting nadir-viewing high-resolution infrared sounder operating in a cross-track-scanning mode. It was launched onboard the EOS Aqua satellite in May 2002, with two operational microwave sounders, AMSU and HSB, and is operational since September 2002. It is a high-spectral resolution, grating multispectral infrared sounder with 2378 channels. Its spectral domain ranges from 650 cm^{-1} to 2665 cm^{-1} ($15.4\text{ }\mu\text{m}$ and $3.8\text{ }\mu\text{m}$), with a



spectral resolving power of 1200 (i.e., a spectral resolution ranging from 0.5 cm^{-1} to 2 cm^{-1}). This domain is divided into three spectral bands, from 650 to 1135 cm^{-1} , from 1215 to 1615 cm^{-1} and from 2180 to 2665 cm^{-1} . AIRS cross-track scanning is 1650 km and covers 70% of the earth every day (Figure 2). The instantaneous field of view (IFOV) is sampled by 3×3 circular pixels whose ground resolution is 13 km at nadir. Measurements from AIRS and AMSU are analyzed jointly to filter out the effects of clouds from the IR data in order to derive various atmospheric and surface variable in clear conditions.

As seen in Figure 2, scanning of both sounders is synchronized, with 9 AIRS fields of view (FOV) (dark yellow circles) embedded in 1 AMSU FOV (light yellow circle with dashed outline), allowing the same atmospheric situation to be simultaneously observed by both instruments.

Figure 2: AIRS and AMSU scan geometrics. (Left) A typical one-day scan pattern of AIRS is shown. (Middle) An artistic view of AIRS and its scan geometry. (Right) AIRS (dark yellow) and AMSU (light yellow) instantaneous fields of view (Jason, 2008).





2. Input and auxiliary data

2.1 Level 1 data

IASI and AMSU input data are Level 1c and Level 1b radiance data respectively, disseminated in near-real time through the EUMETCast system of EUMETSAT. Metop-A data have been available between July 2007 and September 2021 when Metop-A was decommissioned. Metop-B data are available since February 2013. Metop-C data are available since July 2019.

The AIRS and AMSU (onboard the Aqua satellite) input data are both Level 1b radiance data, disseminated in near-real time by NOAA.

2.2 Other data

2.2.1 The TIGR database

The CNRS-LMD Non Linear Inference Scheme (NLIS) used to retrieve mid-tropospheric columns of greenhouse gases is based on artificial neural networks trained on a dataset of well-known atmospheric situations: the Thermodynamic Initial Guess Retrieval (TIGR). In its latest version, available at <https://ara.lmd.polytechnique.fr/index.php?page=tigr>, is a climatological library of 2311 representative atmospheric situations selected by statistical methods from 80,000 radiosonde reports. Each situation is described, from the surface to the top of the atmosphere, by the values of the temperature, water vapour and ozone concentrations on a given pressure grid. For each situation are available the radiances of each IASI/AMSU channel simulated under several conditions of observation (satellite zenith angle, surface characteristics, etc.), as well as the atmospheric transmittances and Jacobians (partial derivatives of the brightness temperature with respect to temperature, gas concentration for H₂O, O₃, CO₂, N₂O, CO, CH₄, surface temperature and emissivity). Radiances, transmittances and Jacobians profiles are generated using the 4A forward radiative transfer model.

2.2.2 The ARSA database

The computation of the radiative biases, which plays a critical role in the retrieval process, is based on the ARSA (Analyzed RadioSoundings Archive) database, which is available at <http://ara.abct.lmd.polytechnique.fr/index.php?page=arsa>. ARSA builds on radiosonde observations made by worldwide distributed radiosonde stations and combines them with surface and other auxiliary observations. Physically coherent quality control tests have been developed to detect and eliminate gross errors: format problems, redundant radiosounding and levels, unrealistic jumps, physically implausible values, temporal and vertical inconsistencies in temperature and dew point temperatures. The current ARSA database (about 6 million elements) starts in January 1979, and is extended onwards, on a monthly basis.



3. Algorithms

3.1 Algorithm for IASI mid-tropospheric CO₂ and CH₄ retrieval

3.1.1 General description

Mid-tropospheric columns of methane (CH₄) and carbon dioxide (CO₂) are retrieved from simultaneous observations of the IASI and AMSU instruments flying together onboard the Metop satellites using a non-linear inference scheme. As described in Crevoisier et al. (2009ab), this scheme is based on artificial neural networks. The weakness of the signal induced on IASI radiances by CO₂ and CH₄ variations, associated with the complexity (in particular its non-Gaussian behavior and the low signal-to-noise ratio) of the relationship between CO₂ or CH₄ concentration and observed radiances, makes it difficult to solve this inverse problem. Therefore, a non-linear inference method, based on the Multilayer Perceptron (MLP) neural network (Rumelhart et al., 1986) with two hidden layers, has been preferred to a more classical one. Introduced to derive tropospheric CO₂ integrated content from TOVS (Chédin et al., 2003), it has been modified to process observations from AIRS and IASI.

The main difficulty in estimating global distribution of CO₂ or CH₄ from infrared sounders comes from the fact that infrared measurements are sensitive to both temperature and CO₂/CH₄ variations. Independent information on temperature is thus needed to allow the separation of these two effects. IASI hyperspectral observations in the thermal infrared, which are sensitive to both temperature and gas concentrations of CO₂ or CH₄ are used in conjunction with microwave observations from the AMSU instruments, only sensitive to temperature, to decorrelate both signals. For CH₄, channels located in the 7.7 μm spectral region are used; for CO₂, channels located in the 15 μm region are used.

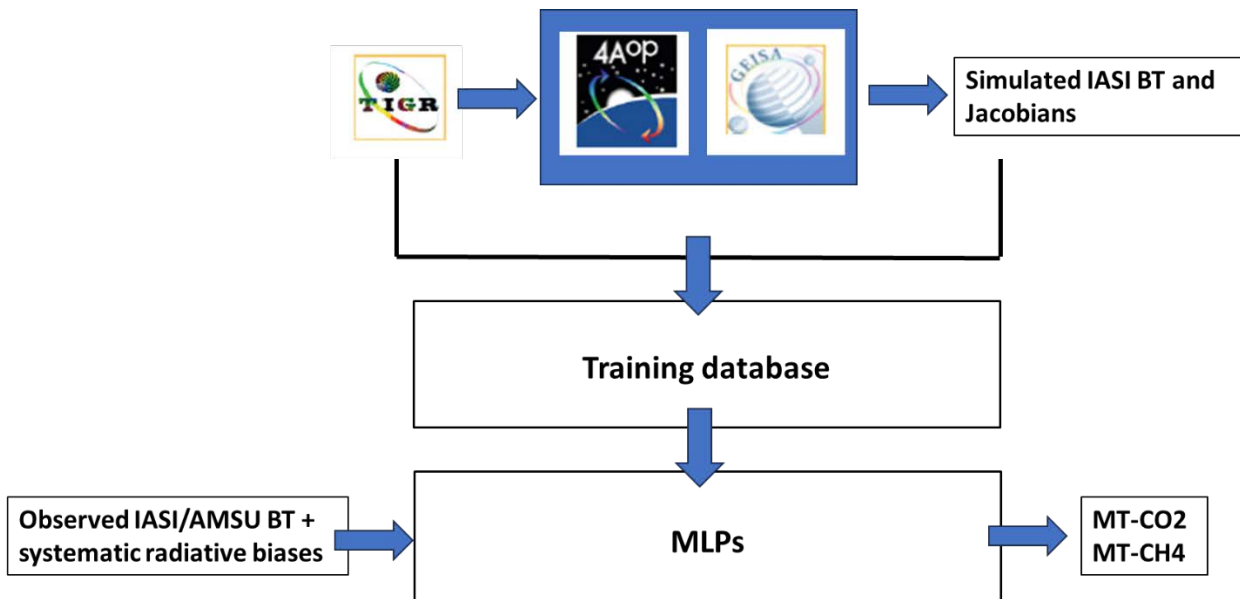
Only a subset of channels presenting the best properties with regards to the retrieval performances, for instance in terms of gas sensitivity and vertical coverage as explained in Crevoisier (2018), are used. The neural networks are trained on a learning dataset with couples of known inputs-outputs coming from the TIGR database and evaluated on an evaluation dataset (the ARSA database). The retrievals are performed during day and night-time (9:30 am/pm local time), both over land and over sea. The CO₂ retrievals are limited to the tropical region (from 30N to 30S); this is because the decorrelation between CO₂ and temperature signals in the IASI radiances is more complex outside of the tropical band due to the higher variability of the temperature profile compared to the tropical one, yielding too high retrieval uncertainty.

Through comparisons with regular aircraft (Machida et al., 2008) or balloon (Membrive et al., 2017) measurements as well as observations made at the surface, we have shown (e.g. Crevoisier et al., 2013) that, once the radiometric characterization of the instruments is performed, IASI and AMSU capture well the trend and interannual variation of CH₄, with an excellent agreement with the rate of increase measured at the surface, giving confidence in the ability of IASI and AMSU to follow its evolution over the 20 years of the Metop program.



Figure 3 shows the different steps between the preparation of the MLPs learning base until the production of the MT-CO₂/CH₄ retrievals.

Figure 3: Flow diagram of the preparation of the learning database and the training of MLPs, and application to IASI/AMSU observations.



3.1.2 Forward model and spectroscopic database

The radiative simulations in the thermal infrared performed in this study are based on the fast and accurate line-by-line radiative transfer model 4A (Automatized Atmospheric Absorption Atlas) (Scott and Chédin, 1981). 4A is an advanced version of the nominal line-by-line STRANSAC model (Scott, 1974) and is basically a compressed look-up-table of optical depths calculated once and for all. It can be coupled to any spectroscopic databases and can simulate any instrumental configurations (ground, airborne, satellite). In addition to the simulation of atmospheric transmissions and radiance (or equivalently brightness temperature (BT)) spectra, 4A analytically computes Jacobians for all relevant atmospheric variables. Jacobians are defined as the partial derivative of the channel brightness temperature with respect to a layer physical variable such as a gas mixing ratio, a temperature or the emissivity. Since the beginning of 2001, an operational version denoted 4A/OP has been developed by the company Noveltis (<https://4aop.noveltis.com/>) in collaboration with CNES and LMD. 4A is the official code chosen by CNES for calibration/validation and preparation activities of several space missions, including IASI and IASI-NG. For this study, the spectrometric parameters used as inputs to 4A, are taken from the GEISA-2011 database (Jacquinet-Husson et al., 2011).

3.1.3 Channel selection



IASI presents 8461 channels covering most of the infrared spectrum. Approximately a hundred of them are sensitive to methane, whilst a few hundred are sensitive to CO₂.

3.1.3.1 Channels for CH₄

IASI channels sensitive to methane are either located in band ν_4 of methane, around 7.7 μm (1306 cm^{-1}), or in band ν_3 , around 3.8 μm (2630 cm^{-1}), and have different sensitivities to methane and other atmospheric or surface components. The sensitivity to methane concentration variations of channels located in the 3.8 μm band is much lower than that of channels located in the 7.7 μm band due to weaker absorption lines: they won't be considered here. In the 7.7 μm band, channels are sensitive to water vapour (H₂O), nitrous oxide (N₂O) and surface characteristics.

The main interference, as far as CH₄ is concerned, comes from H₂O, which dominates the infrared spectrum in methane absorption bands. Since water vapour variability is quite high, especially in the tropics, and knowledge of its tropospheric distribution still limited, separating the CH₄ signal from water vapour is quite challenging and precludes the use of most of the channels. Due to much lower water vapour content in the mid-latitude regions as opposed to the tropics, the interferences between H₂O and CH₄ is less pronounced in the extra-tropical regions, giving access to more channels with a high signal-to-interference ratio. Altogether, only a few successive channels located in the 1301-1303 cm^{-1} interval present a low-enough sensitivity to water vapour to be used to retrieve methane.

24 channels have been selected to optimize the signal-to-interference ratio. They are not sensitive to variations of methane in two parts of the atmosphere: the lower troposphere (roughly below 500 hPa) and the tropopause (Crevoisier et al., 2003). The Jacobians of the selected channels have very similar shapes and all peak around 260 hPa. Hence, IASI only allows the retrieval of a mid-tropospheric column of methane. It is equivalent to say that IASI observations are characterized by only one degree of freedom for CH₄ along the vertical.

3.1.3.2 Channels for CO₂

IASI channels sensitive to carbon dioxide are either located in band ν_2 of CO₂, around 15 μm (670 cm^{-1}), or in band ν_3 , around 4.3 μm (2260 cm^{-1}), and present various sensitivities to methane and other atmospheric or surface components. The 4.3 μm band is characterized by a very high radiometric noise that precludes using this channel for retrieving CO₂. The main interference, as far as CO₂ is concerned, comes from H₂O and ozone. Consequently, use is made of a few successive channels located in the 670 cm^{-1} interval.

These channels are not sensitive to variations of CO₂ in two parts of the atmosphere: the lower troposphere (roughly below 500 hPa) and the tropopause (Crevoisier et al., 2003). The Jacobians of the selected channels have very similar shapes and all peak around 200 hPa. Hence, IASI only allows the retrieval of a mid-tropospheric column of carbon dioxide. It is equivalent to say that IASI observations are characterized by only one degree of freedom on the vertical for CO₂.



3.1.4 Neural architecture

The weakness of the signal induced on IASI brightness temperature (BT) by CH₄ or CO₂ variations, associated with the complexity (in particular its non-Gaussianity) of the relationship between the gas concentration and observed BT, makes it difficult to solve this inverse problem. To tackle this problem, use is made of a non-linear inference method, based on the Multilayer Perceptron (MLP) neural network (Rumelhart et al., 1986) with two hidden layers. Following the selection of IASI and AMSU channels described previously, the chosen neural architectures are the following.

3.1.4.1 Architecture for CH₄

- Until version 8.4

The input layer is composed of:

- (i) 24 IASI BT. Among them, the first 5 channels are not sensitive to CH₄ but to stratospheric temperature only. They have been included in order to deal with the slight sensitivity of the selected CH₄ IASI channels to stratospheric temperature;
- (ii) 2 AMSU BT of channels 6 and 8;
- (iii) 10 differences between IASI and AMSU BT, to help constraining the convergence process: 6-2497, 8-2497, 6-2553, 8-2553, 6-2634, 8-2634, 6-2637, 8-2637, 6-2809, 8-2809.

Altogether, there are 36 predictors.

The output layer of the network is composed of:

- (i) the difference between the true value of CH₄ concentration (associated with inputs) and the TIGR reference one (1860 ppb);
- (ii) 24 differences between the “true” IASI BT (associated with the true CH₄ concentration value) and the “reference” one (associated with the reference CH₄ concentration value), once again to constrain the solution.

Altogether, there are 25 predictands.

Our past experience and several trials have led us to choose 70 neurons for the first hidden layer and 40 for the second one.

- Version 9.1

In order to be able to process the entire time series of IASI-A and IASI-B data with the same retrieval code and obtain a homogeneous data set of mid-tropospheric CH₄ from both instruments, a new architecture has been used to process the observations. This new version 9.1 copes with the failure of AMSU8 channels on Metop-A in 2015 by removing the use of this channel for all Metop satellites.

The input layer is now composed of: (i) 24 IASI BT. Among them, the first 5 channels are not sensitive to CH₄ but to stratospheric temperature only. They have been included in order to deal



with the slight sensitivity of the selected CH₄ IASI channels to stratospheric temperature; (ii) 1 AMSU BT of channel 6; (iii) 5 differences between IASI and AMSU BT, to help constraining the convergence process : 6-2497, 6-2553, 6-2634, 6- 2637, 6-2809. Altogether, there are 30 predictors.

The output layer of the network is composed of: (i) the difference between the true value of CH₄ concentration (associated with inputs) and the TIGR reference one (1860 ppb); (ii) 14 differences between the “true” IASI BT (associated with the true CH₄ concentration value) and the “reference” one (associated with the reference CH₄ concentration value), once again to constrain the solution. Altogether, there are 15 predictands.

The hidden layers are still made up of 70 neurons for the first layer and 40 for the second one.

- Version 10.2

Two changes of the NLIS algorithm have been made for this new version. First, use has been made of the improved version of 4A/OP (v1.7, released end of 2021), that includes improvements in spectroscopy and radiative transfer physics. This has required recomputing the spectral radiative biases over the lifetime of all three Metop satellites. Second, in order to account for the strong increase in CH₄ atmospheric mixing ratio since the beginning of Metop-A observations in 2007, a larger range of variation of CH₄ (1860 ± 250 ppb) has been used in the training phase. These values will insure that the NLIS algorithm will cope with the planned future increase of CH₄ mixing ratio until the end of Metop-C. The neural architecture of the NLIS algorithm is the same as in version 9.1.

3.1.4.2 Architecture for CO₂

- Until version 8.n

The input layer is composed of:

- 89 IASI BT. Among them, the first 5 channels are not sensitive to CO₂ but to stratospheric temperature only. They have been included in order to deal with the slight sensitivity of the selected CO₂ IASI channels to stratospheric temperature;
- 2 AMSU BT of channels 6 and 8;
- 10 differences between IASI and AMSU BT, to help constraining the convergence process.

Altogether, there are 101 predictors.

The output layer of the network is composed of:

- the difference between the true value of CO₂ concentration (associated with inputs) and the TIGR reference one (372 ppm);
- 24 differences between the “true” IASI BT (associated with the true CO₂ concentration value) and the “reference” one (associated with the reference CO₂ concentration value), once again to constrain the solution.

Altogether, there are 25 predictands.



Our past experience and several trials have led us to choose 70 neurons for the first hidden layer and 40 for the second one.

- Version 9.1

In order to be able to process the entire time series of IASI-A and IASI-B data with the same retrieval code and obtain a homogeneous data set of mid-tropospheric CO₂ from both instruments, a new architecture has been used to process the observations. This new version 9.1 copes with the failure of AMSU8 channels on Metop-A in 2015 by removing the use of this channel for all Metop satellites.

The input layer is now composed of:

- (i) 84 IASI BT;
- (ii) 1 AMSU BT of channel 6;
- (iii) 8 differences between IASI and AMSU BT, to help constraining the convergence process: 6-199, 6-205, 6-207, 6-208, 6-211, 6-214, 6-222, 6-299.

Altogether, there are 93 predictors.

The output layer of the network is composed of:

- (i) the difference between the true value of CO₂ concentration (associated with inputs) and the TIGR reference one (372 ppm);
- (ii) 84 differences between the “true” IASI BT (associated with the true CH₄ concentration value) and the “reference” one (associated with the reference CH₄ concentration value), once again to constrain the solution.

Altogether, there are 85 predictands.

The hidden layers are still made up of 70 neurons for the first layer and 40 for the second one.

- Version 10.2

Two changes of the NLIS algorithm have been made for this new version. First, use has been made of the improved version of 4A/OP (v1.7, released end of 2021), that includes improvements in spectroscopy and radiative transfer physics. This has required recomputing the spectral radiative biases over the lifetime of all three Metop satellites. Second, in order to account for the strong increase in CO₂ atmospheric mixing ratio since the beginning of Metop-A observations in 2007, a larger range of variation of CO₂ has been used in the training phase. This will insure that the NLIS algorithm will cope with the planned future increase of CO₂ mixing ratio until the end of Metop-C. The neural architecture of the NLIS algorithm is the same as in version 9.1.

3.1.5 Training of the networks

The learning algorithm is the optimization technique that estimates the optimal network parameters by minimizing a positive-definite cost function which measures, for a set of representative situations for which inputs (here the brightness temperatures) and outputs (gas) are known (the learning set), the mismatch between the neural network outputs and the desired



outputs. Here, the Error Back-Propagation algorithm (Rumelhart et al., 1986) is used to minimize the cost function. It is a gradient descent algorithm well adapted to the MLP hierarchical architecture because the computational cost is linearly related to the number of parameters. To avoid being trapped in local minima during the minimization of the cost function, stochastic steepest descent is used. The learning step is made sample by sample, chosen iteratively and stochastically in the learning data set.

The training database from which the networks learn the relationship existing between inputs and outputs is based on the TIGR database. For all TIGR atmospheric situations, for all scan angles, and for the whole IASI channels used in the retrieval process, clear-sky brightness temperatures, transmittances and Jacobians have been computed using the 4A/OP radiative transfer model with the spectroscopic database GEISA-2011 as input. The required AMSU BTs are computed using the STRANSAC microwave forward model. Network input BTs correspond to randomly drawn values of concentration in the range 1760-1960 ppb for CH₄ and in the range 362-382 ppm for CO₂, centred on the TIGR reference value of 1860 ppb for CH₄ and 372 ppm for CO₂; they are computed using the stored CH₄ and CO₂ Jacobians. It is worth noting that no prior information is thus given to the networks in terms of seasonality, trend, or geographical patterns of the gases.

Neural networks are trained for each of the 15 AMSU scan angles and for 2 air-masses (tropical or mid-latitude) independently. Surface elevation is also taken into account. Altogether, for a given neural architecture, 240 networks are trained. For each network corresponding to one air-mass, one scan angle and one surface type, the learning steps are the following:

- 1) One atmosphere is randomly chosen among the TIGR atmospheres of the considered air-mass.
- 2) A CH₄ (resp. CO₂) mixing ratio is drawn randomly (uniform distribution) in the range 1760-1960 ppb (resp. 362-382 ppm), which is centred on the reference CH₄ (resp. CO₂) mixing ratio of TIGR.
- 3) A perturbation of the surface temperature is randomly chosen according to the normal distribution, with a null mean value and a standard deviation of 4 K.
- 4) The input BTs at the drawn CH₄ (resp. CO₂) mixing ratio are computed using BTs and CH₄ (resp. CO₂) Jacobians from TIGR for the considered atmosphere.
- 5) For IASI channels, noise equivalent temperatures are computed at the BT according to Eq. 1:

$$NE\Delta T[T_B(\nu), \nu] = NE\Delta T[T_{ref}, \nu] \frac{\frac{\partial B}{\partial T}(T_{ref}, \nu)}{\frac{\partial B}{\partial T}(T_B(\nu), \nu)} \quad (1)$$

where NE ΔT is the equivalent noise temperature taken at the brightness temperature T_B , of the channel located at frequency ν , and B is the radiance. The reference noise corresponding to a reference temperature T_{ref} of 280 K is taken from the in-flight noise measurement (CNES, priv. comm.). To increase the signal to noise ratio, and speed the learning phase, these noises have been divided by 2. Since 4 IASI spots are localized within one AMSU spot, the average of IASI BT contained in a single AMSU field-of-view are therefore used as inputs to the networks.

- 6) The quadratic sum of the instrument noise and the forward radiative transfer model noise, are computed and added to the BT.



- 7) The inputs and outputs are normalized in order to homogenise the input values between 0 and 1.
- 8) The Error Back-Propagation algorithm (Rumelhart et al., 1986) is used to minimize the cost function.
- 9) The parameters of the networks are updated.
- 10) The networks are applied to the whole ARSA atmospheres following the same procedure as TIGR (steps 4 to 7) and the root mean square (RMS) error of the output is computed.
- 11) Go back to step 1, until the predefined number of iterations has been reached.



3.1.6 Application to observations

3.1.6.1 General description

Once the learning phase is completed, observations of IASI and AMSU can be used to infer mid-tropospheric columns of CH₄ or CO₂. The retrieval is performed at the AMSU resolution: when 4 IASI FOVs included in 1 AMSU FOV are declared clear (meaning that no cloud nor aerosol has been detected), the BTs of the channels are averaged over the 4 IASI FOVs and used together with AMSU BTs, to perform the retrieval.

Since the networks are trained with simulated data, potential systematic radiative biases existing between simulations used in the learning phase and observations must be removed before using these BTs as inputs to the network corresponding to the situation according to the scan angle, surface elevation and air-mass type. These systematic radiative biases are computed with the calibration/validation chain that has been developed for many years at LMD (Armante et al., 2016). For each channel, the differences between simulations and collocated (in time and space) satellite observations are averaged over several full years of operation. These differences are called 'calc-obs' residuals. The simulations are performed using the 4A/OP forward model and radiosonde measurements from ARSA as inputs. One key element is that, during this computation, the CH₄ and CO₂ mixing ratios are kept at the reference value of the TIGR database (1860 ppb and 372 ppm respectively) to avoid making the CH₄ nor CO₂ signals disappearing in the BT used as input to the networks. Every month, about 100 collocations are available, giving access to robust statistics.

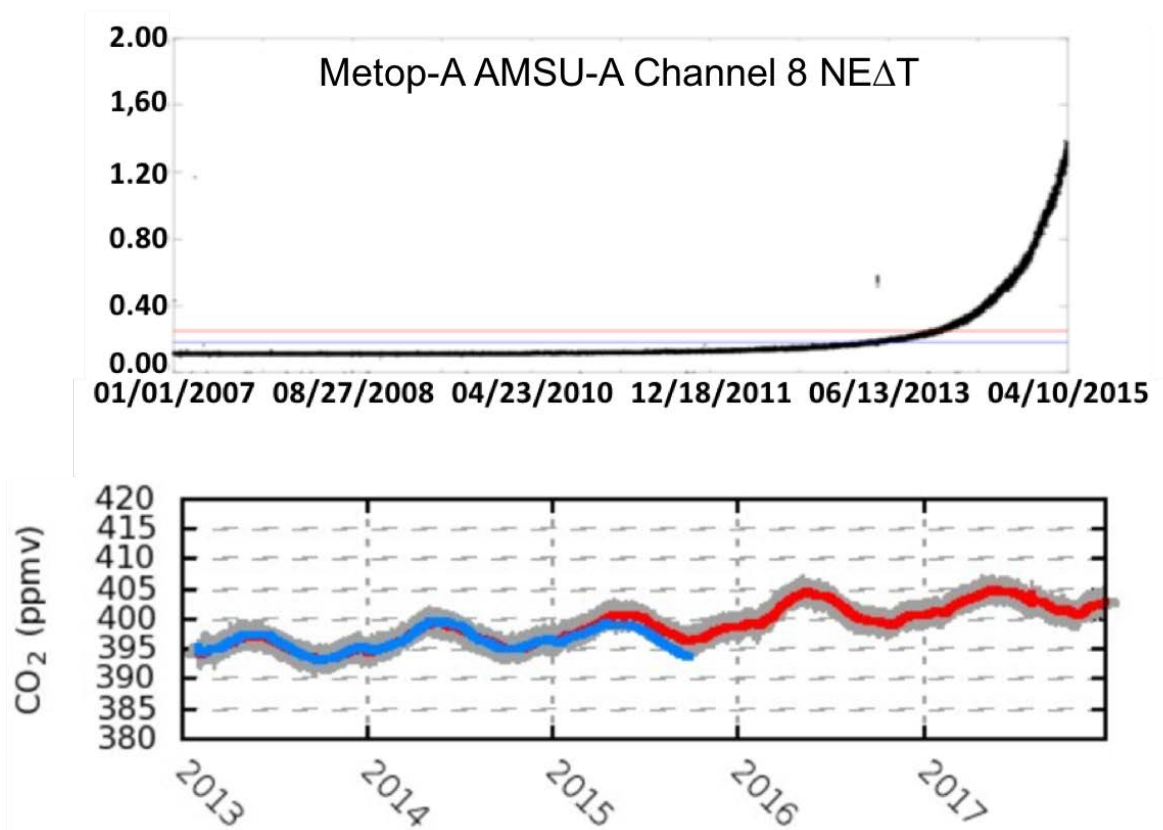
By averaging thousands of situations together, it is possible to derive the change in the averaged biases with the scan angle. In order to avoid potential biases due to the incorrect modelling of the radiative effect of scan angles close to the edges of the orbit, which is particularly the case for microwave observation, specific radiative biases have to be taken into account for each scan angle.



3.1.6.2 Case of Metop-A from 2015

From the beginning of 2015, some channels of AMSU onboard Metop-A, including channel 8, started degrading, and subsequently became out of nominal specifications and were finally declared non-operational by the end of the year. The continuous degradation of channel 8 had a direct impact on the CO₂ and CH₄ time series derived from Metop-A as seen in Fig. 4.

Figure 4: (Top) AMSU channel 8 Ne Δ T from January 2007 to October 2015. Red and blue horizontal lines show noise specification pre and post launch (Bottom) Mid-tropospheric CO₂ derived from Metop-A (blue) and from Metop-B (red) from February 2013 to December 2017. Although the agreement between Metop-A and Metop-B CO₂ is excellent between February 2013 and May 2015, an increasing bias between the 2 products can be clearly seen from June up to the end of Metop-A/AMSU channel 8 in October 2015.



Following the degradation, a full characterization of the spectral and radiometric characteristics of AMSU onboard Metop-A has been carried on to evaluate its impact on the retrieval. It has been found that the degradation had the largest impact after June 2015 and that no correction could be applied for the following months to correct the very large drift of AMSU channel 8 (Fig. 4 left). Several attempts to find proper replacements for AMSU 8 channel have then been made. The



optimal scenario (lowest impact on both bias and uncertainty) has been found to be using channel 6 only (see section 3.1.4)

As of version 9.1, AMSU 8 channel is no longer used in the retrieval scheme and a full reprocessing of the Metop-A time series has been made.

3.1.6.3 Case of Metop-B from August 2nd 2017

On August, 2nd 2017, the on-board processing of IASI/Metop-B changed, due to the update of the correction of the non-linearity of detectors. This change had a noticeable impact on IASI spectral band 1 where the channels used to retrieve CO₂ are located. Typically, it induced a 0.2 K bias in the measured brightness temperatures, which corresponds to a bias of about 5 ppm. To deal with this problem, a new set of radiative biases have been computed for IASI/Metop-B. The radiative bias corresponding to the August 2nd change has been computed by comparing the 'calc-obs' residuals computed over 1 month after and before the change. Atmospheric situations were taken from ECMWF analyses collocated in time and space with IASI/Metop-B. Depending on the date, a different set of radiative biases must now be considered before and after August 2nd for the processing of IASI/Metop-B.

As of version 9.1, AMSU 8 channel is no longer used in the retrieval scheme and a full reprocessing of the Metop-B time series has been made.

3.1.6.4 Case of Metop-A from September 30th 2019

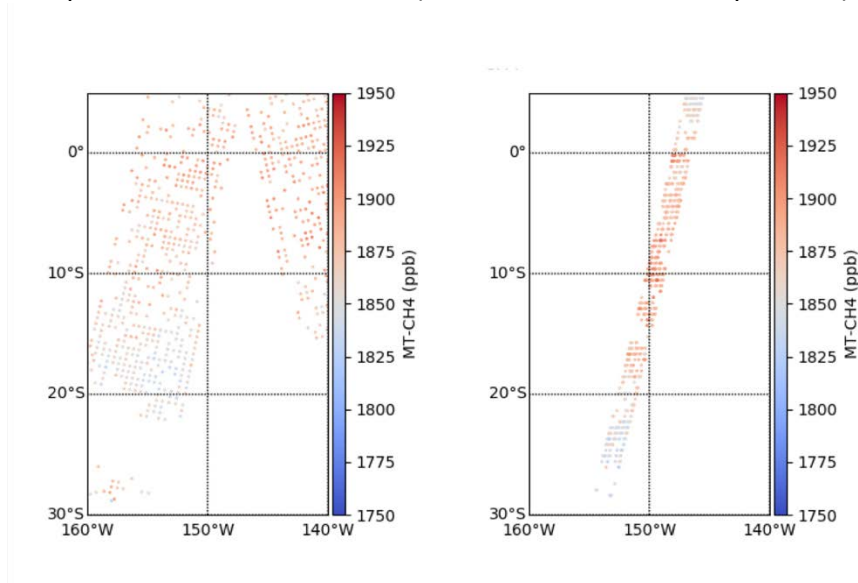
On September 30th 2019, the on-board processing of IASI/Metop-A changed, due to the update of the correction of the non-linearity of detectors. This change at instrument level had a noticeable impact on IASI spectral band 1 where the channels used to retrieve CO₂ are located. Typically, it induced a 0.1 K bias in the measured brightness temperatures, which correspond to a bias of about 2 ppm that is seen in the retrieval. This change has been fully characterized at Level 1 and implemented in the retrieval process.



3.1.6.5 Case of Metop-A between September 15th and October 15th 2021

As part of end-of-life scenarios for Metop-A that have been implemented by EUMETSAT and CNES, the IASI instrument has been turned to a ‘super-sampled mode’: as seen in Fig 5, all FOVs that usually cover a swath of 2 200 km (left) were now covering a swath of 220 km only (right), with a typical distance between two consecutive FOVs of less than 2km. The processing chains developed at LMD were able to cope with this situation and all retrievals have been performed smoothly.

Figure 5: (Left) Nominal swath of IASI (here MT-CH4 on 24th Sept. 2020). (Right) Oversampling mode of IASI-A between Sept. 15th and Oct. 15th 2021 (here MT-CH4 on 24th Sept. 2022).





3.1.7 Vertical characterization of the retrieval

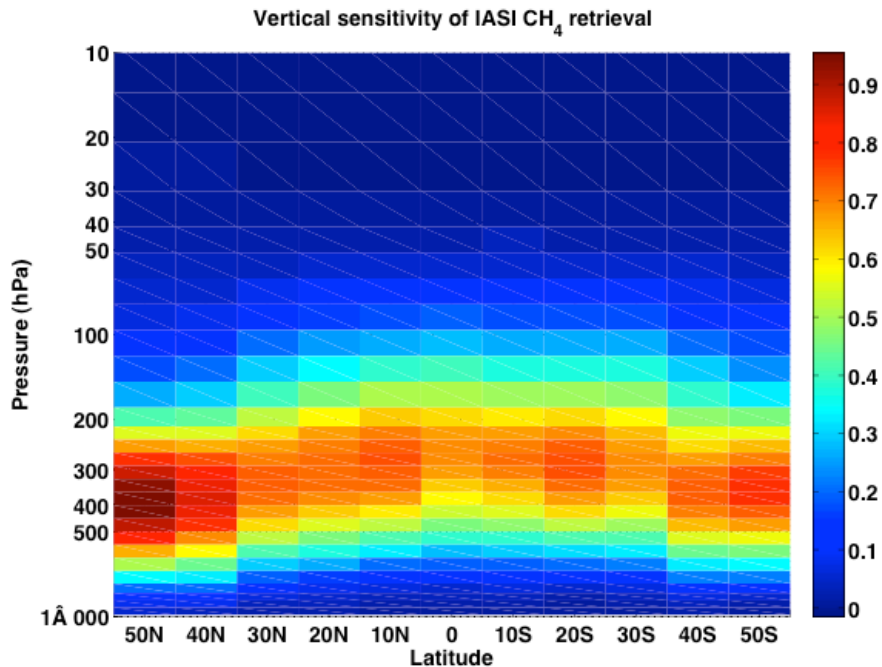
As stated before, IASI channels located in the 7.7 μm and 15 μm bands are mostly sensitive to tropospheric variations of gases. The averaging kernels, which indicate which part of the atmosphere the retrievals are representative of, are determined through radiative transfer simulations. A uniform perturbation of CH_4 or CO_2 mixing ratio is applied sequentially to each of the 40 pressure layers used in ARSA to characterize atmospheric profiles. IASI and AMSU brightness temperatures are then computed for each of the perturbed atmospheric profiles and used as inputs to the neural networks. The theoretical change F_i in ppbv/ppbv of the column mean apparent mixing ratio (\hat{q}) given a mixing ratio perturbation of dq^{ref} at level i , is then given by

$$F_i = \frac{\hat{q}(\Delta q_i - dq^{ref}) - \hat{q}(\Delta q_i - 0)}{dq^{ref}} \quad (2)$$

The mean of the averaging kernel for CH_4 computed over the ARSA dataset is plotted in Fig. 6. In the tropics, the height of the tropopause is approximately 17 km, whereas it is closer to 8km in the mid-latitudes. The non-linear inference scheme gives access to a mid-to-upper tropospheric integrated content of CH_4 covering: (i) the range 100-500 hPa (roughly 9-15 km), with the highest sensitivity around 230 hPa in the tropics; (ii) the range 250-700 hPa (roughly 6-12 km), with the highest sensitivity around 400 hPa in the mid-latitudes.



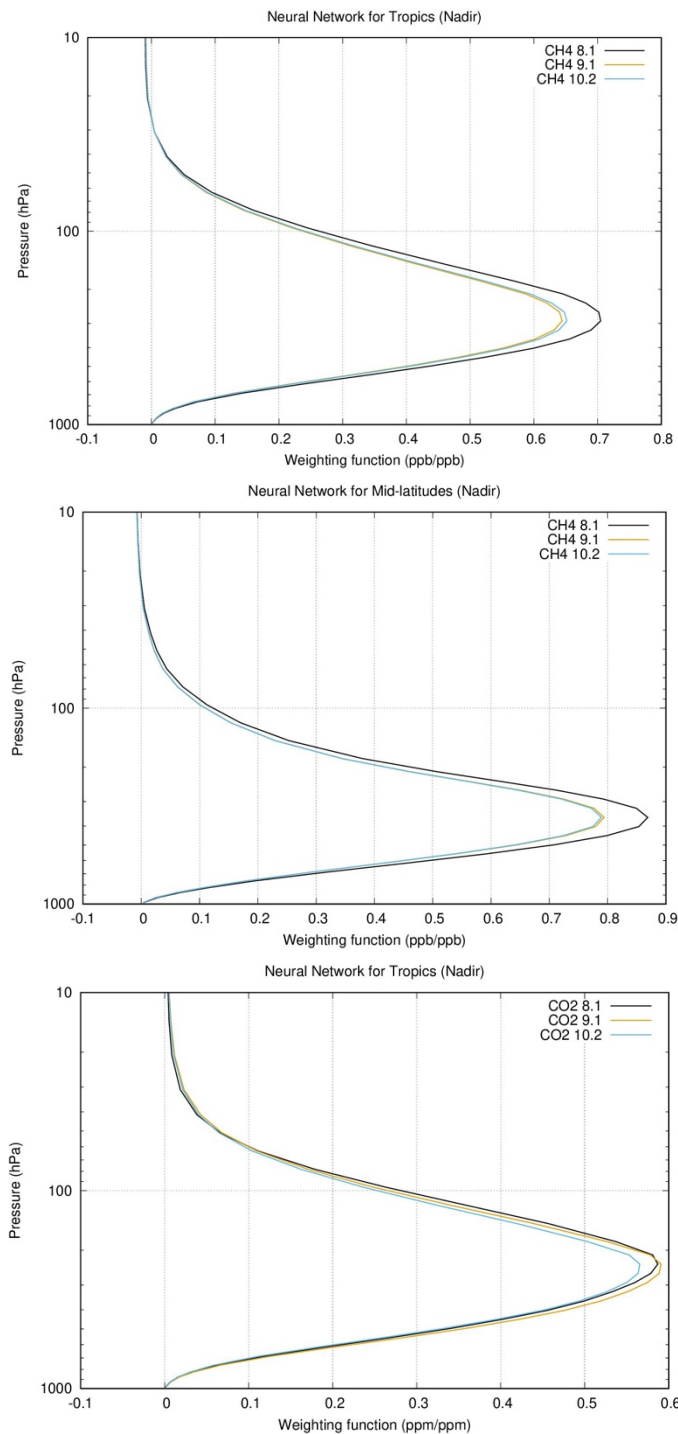
Figure 6: Vertical sensitivity of IASI CH₄ retrievals (until V8.4) as a function of latitude.



Since the AMSU channel (8) is no longer used in the retrieval process in version 9.1, the vertical sensitivities of CH₄ retrievals slightly changed, as shown in Figure 7. Since the only AMSU channel (6) that is used is a tropospheric channel, the sensitivity is slightly increased in the troposphere compared to previous versions. However, since versions 9.1 and 10.2 use the same channels, their weighting functions are almost identical, the slight changes between the two coming from the use of two different versions of 4A/OP.



Figure 7: Averaged vertical sensitivity of IASI CH₄ (in the mid-latitudes, top, and in the tropics, middle) and CO₂ retrievals (bottom) before (orange) and after (green) version 9.1 and for version 10.2 (black).





3.2 Algorithm for AIRS mid-tropospheric CO₂ retrieval

3.2.1 General description

Mid-tropospheric columns of carbon dioxide (CO₂) are retrieved from simultaneous observations of the AIRS and AMSU instruments flying together onboard the Aqua satellite using a first version of the non-linear inference scheme used for processing IASI and AMSU data as described in Section 3.1. This inference scheme is based on Multi-Layer Perceptron artificial neural networks with 2 hidden layers. AIRS hyperspectral observations in the thermal infrared at 15 and 4.3 μm, which are sensitive to both temperature and gas concentrations of CO₂, are used in conjunction with microwave observations from the AMSU instruments, only sensitive to temperature, to decorrelate both signals.

Only a subset of channels presenting the best properties with regards to the retrieval performances are used. The neural networks are trained on a learning dataset with couples of known inputs-outputs (TIGR). As opposed to the processing of IASI and AMSU observations from the Metop series, no continuous evaluation of the neural networks performance throughout the training has been performed. The retrievals are performed during day and night-time (1:30 am/pm local time), both over land and over sea. The CO₂ retrievals are limited to the tropical region (25N:25S).

Through comparisons with regular aircraft (Machida et al., 2008) measurements, it has been shown that, once the radiometric characterization of the instruments is performed, AIRS and AMSU capture well the trend and interannual variation of CO₂, until the loss of some of channels used in the retrieval process in July 2007. The retrieval of CO₂ from AIRS has been stopped ever since.

3.2.2 Forward model and spectroscopic database

The radiative simulations in the thermal infrared performed in the retrieval process are based on fast and accurate line-by-line radiative transfer model 4A (Automatized Atmospheric Absorption Atlas) (Scott and Chédin, 1981). 4A is an advanced version of the nominal line-by-line STRANSAC model (Scott, 1974) and is basically a compressed look-up-table of optical depths calculated once and for all. It can be coupled to any spectroscopic databases and can simulate any instrumental configurations (ground, airborne, satellite). In addition to the simulation of atmospheric transmissions and radiance (or equivalently brightness temperature) spectra, 4A analytically computes Jacobians for all relevant atmospheric variables. Jacobians are defined as the partial derivative of the channel brightness temperature with respect to a layer physical variable such as a gas mixing ratio, a temperature or the emissivity. Since the beginning of 2001, an operational version denoted 4A/OP has been developed by Noveltis (<https://4aop.noveltis.com/>) in collaboration with CNES and LMD. 4A is the official code chosen by CNES for calibration/validation and preparation activities of several space missions, including IASI and IASI-NG. For generating AIRS CO₂, the spectrometric parameters used as inputs to 4A, are taken from the GEISA-2008 database (Jacquinet-Husson et al., 2009).



3.2.3 Channel selection

AIRS presents 2378 channels covering most of the infrared spectrum. Only a few hundred of them are sensitive to CO₂. They are either located in band ν_2 of CO₂, around 15 μm (670 cm^{-1}), or in band ν_3 , around 4.3 μm (2260 cm^{-1}), and present various sensitivities to CO₂ and other atmospheric or surface components. As opposed to IASI, the AIRS channels located in the 4.3 μm band are characterized by a radiometric noise of the same order as for the channels located at 15 μm , which means that both CO₂ absorption bands are used to perform the retrieval. As will be detailed in Section 3.2.7, the use of channels located at 4.3 μm yields a sensitivity to CO₂ at lower altitudes than for IASI. The main interference, as far as CO₂ is concerned, comes from H₂O and ozone.

A set of AIRS and AMSU channels presenting optimal characteristics to estimate CO₂ has been selected in Crevoisier et al. (2003) prior to the launch of the Aqua satellite. Based on increasing experience with the instruments, the channel selection has been refined, based on three criteria: (1) their sensitivity to CO₂; (2) their sensitivity to other atmospheric components, as well as to surface characteristics; and (3) to their sensitivity to variation of CO₂ along the vertical. A set of 15 channels has been selected; 9 of them are located in the 15 μm band (channels 173, 175, 180, 185, 193, 213, 218 and 250), the other being located in the 4.3 μm band.

These channels are not sensitive to variations of CO₂ in two parts of the atmosphere: the lower troposphere (roughly below 500 hPa) and the tropopause (Crevoisier et al., 2003). The Jacobians of the selected channels have very similar shapes and all peak around 200-300 hPa. Hence, AIRS only allows the retrieval of a mid-tropospheric column of carbon dioxide. It is equivalent to say that AIRS observations are characterized by only one degree of freedom on the vertical for CO₂.

3.2.4 Neural architecture

The weakness of the signal induced on AIRS brightness temperature (BT) by CO₂ variations, associated with the complexity (in particular its non-Gaussianity) of the relationship between the gas concentration and observed BT, makes it difficult to solve this inverse problem. To tackle this problem, use is made of a non-linear inference method, based on the Multilayer Perceptron (MLP) neural network (Rumelhart et al., 1986) with two hidden layers. Following the selection of AIRS and AMSU channels described previously, the chosen neural architectures are the following.

The input layer is composed of:

- (i) 15 AIRS BT;
- (ii) 2 AMSU BT of channels 6 and 8 ;
- (iii) 15 differences between the 15 AIRS channels and AMSU 6 BT, to help constraining the convergence process.

Altogether, there are 32 predictors.

The output layer of the network is composed of:



- (i) the difference between the true value of CO₂ concentration (associated with inputs) and the TIGR reference one (372 ppm);
- (ii) 24 differences between the “true” AIRS BT (associated with the true CO₂ concentration value) and the “reference” one (associated with the reference CO₂ concentration value), once again to constrain the solution.

Altogether, there are 16 predictands. The first and second hidden layers are made of 70 and 40 neurons, respectively.

3.2.5 Training of the networks

The learning algorithm is the optimization technique that estimates the optimal network parameters by minimizing a positive-definite cost function which measures, for a set of representative situations for which inputs (here the brightness temperatures) and outputs (gas) are known (the learning set), the mismatch between the neural network outputs and the desired outputs. Here, the Error Back-Propagation algorithm (Rumelhart et al., 1986) is used to minimize the cost function. It is a gradient descent algorithm well adapted to the MLP hierarchical architecture because the computational cost is linearly related to the number of parameters. To avoid being trapped in local minima during the minimization of the cost function, stochastic steepest descent is used. The learning step is made sample by sample, chosen iteratively and stochastically in the learning data set.

The training database from which the networks learn the relationship existing between inputs and outputs is based on the TIGR database. For all TIGR atmospheric situations, for all scan angles, and for the whole IASI channels used in the retrieval process, clear-sky brightness temperatures (BT), transmittances and Jacobians have been computed using the 4A/OP radiative transfer model with the spectroscopic database GEISA-2011 as input. The required AMSU BTs are computed using the STRANSAC microwave forward model. Network input BTs correspond to randomly drawn values of CO₂ concentration among the values [362:4:382] ppm, centered on the TIGR reference value of 372 ppm; they are computed using the stored CO₂ Jacobians. It is worth noting that no prior information is thus given to the networks in terms of seasonality, trend, or geographical patterns of the gases.

Neural networks are trained for each of the 10 first AMSU scan angles and for tropical situations, independently. Surface elevation is also taken into account. All together, for a given neural architecture, 80 networks are trained. For each network corresponding to one air-mass, one scan angle and one surface type, the learning steps are the following:

- 1) One atmosphere is randomly chosen among the TIGR atmospheres of the considered air-mass.
- 2) A CO₂ mixing ratio is drawn randomly among the values [362:4:382] ppm, centered on the reference CO₂ mixing ratio of TIGR.
- 3) A perturbation of the surface temperature is randomly chosen according to the normal distribution, with a null mean value and a standard deviation of 4 K.
- 4) The input BTs at the drawn CO₂ mixing ratio are computed using BTs and CO₂ Jacobians from TIGR for the considered atmosphere.



- 5) For AIRS channels, noise equivalent temperatures are computed at the BT according to Eq. 1:

$$NE\Delta T[T_B(\nu), \nu] = NE\Delta T[T_{ref}, \nu] \frac{\frac{\partial B}{\partial T}(T_{ref}, \nu)}{\frac{\partial B}{\partial T}(T_B(\nu), \nu)} \quad (3)$$

where $NE\Delta T$ is the equivalent noise temperature taken at the brightness temperature T_B , of the channel located at frequency ν , and B is the radiance. The reference noise corresponding to a reference temperature T_{ref} of 280 K is taken from the in-flight noise measurement. To increase the signal to noise ratio, and speed the learning phase, these noises have been divided by 3. Since 9 IASI spots are localized within one AMSU spot, the average of IASI BT contained in a single AMSU field-of-view are therefore used as inputs to the networks.

- 6) The quadratic sum of the instrument noise and the forward radiative transfer model noise, are computed and added to the BT.
- 7) The inputs and outputs are normalized in order to homogenise the input values between 0 and 1.
- 8) The Error Back-Propagation algorithm (Rumelhart et al., 1986) is used to minimize the cost function.
- 9) The parameters of the networks are updated.
- 10) Come back to step 1, until the predefined number of iterations has been reached.

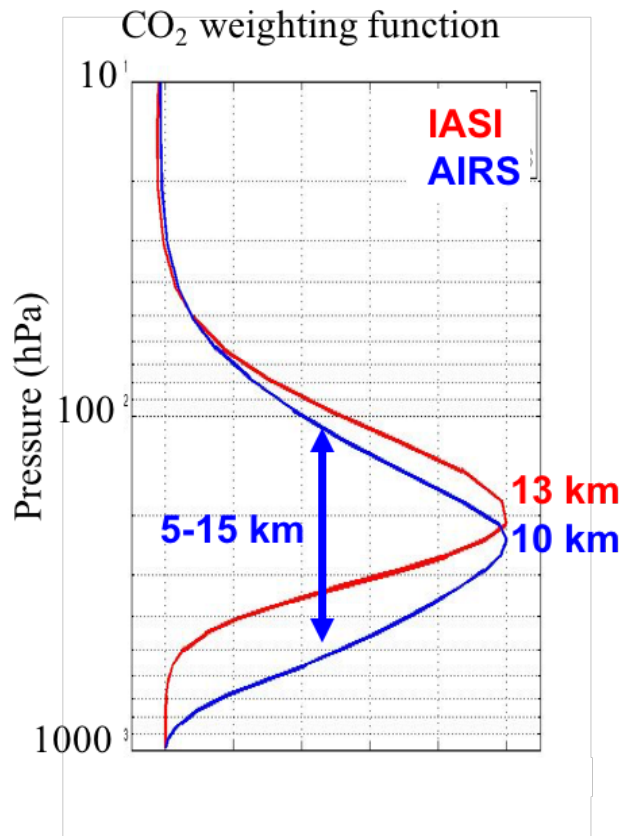
3.2.6 Application to observations

Once the learning phase is completed, observations of AIRS and AMSU can be used to infer mid-tropospheric columns of CO_2 . The retrieval is performed at the AMSU resolution: when 9 AIRS FOVs included in 1 AMSU FOV are declared clear (meaning that no cloud nor aerosol has been detected), the BTs of the channels are averaged over the 9 AIRS FOVs and used together with AMSU BTs, to perform the retrieval.

Since the networks are trained with simulated data, potential systematic radiative biases existing between simulations used in the learning phase and observations must be removed before using these BTs as inputs to the network corresponding to the situation according to the scan angle, surface elevation and air-mass type. These systematic radiative biases are computed with one of the first version of the calibration/validation chain that has been developed for many years at LMD. For each channel, the differences between simulations and collocated (in time and space) satellite observations were averaged over 5 years of operation. These differences are called 'calc-obs' residuals. The simulations were performed using the 4A/OP forward model and radiosonde measurements from the ECMWF database as inputs. One key element is that, during this computation, CO_2 mixing ratio is kept at the reference value of the TIGR database (372 ppm) to avoid making the CO_2 signal disappear in the BT used as input to the networks. Every month, about 100 collocations were available, giving access to robust statistics. No scan-angle was applied to the biases, restricting the retrieval to the 10 smallest AMSU scan angle.



Figure 8: AIRS and IASI CO₂ averaging kernel computed over the TIGR tropical atmospheric situations.





3.2.7 Vertical characterization of the retrieval

As stated before, AIRS channels located in the 15 and 4.3 μm bands are mostly sensitive to tropospheric variations of gases. The averaging kernels, which indicate which part of the atmosphere the retrievals are representative of, are determined through radiative transfer simulations. A uniform perturbation of CO_2 mixing ratio is applied sequentially to each of the 40 pressure layers used in TIGR to characterize atmospheric profiles. AIRS and AMSU brightness temperatures are then computed for each of the perturbed atmospheric profiles and used as inputs to the neural networks. The theoretical change F_i in ppm/ppm of the column mean apparent mixing ratio (\hat{q}) given a mixing ratio perturbation of dq^{ref} at level i , is then given (Crevoisier, 2004) by

$$F_i = \frac{\hat{q}(\Delta q_i - dq^{ref}) - \hat{q}(\Delta q_i - 0)}{dq^{ref}} \quad (4)$$

The mean of the averaging kernel for CO_2 computed over the TIGR dataset is plotted in Fig. 8. The non-linear inference scheme gives access to a mid-to-upper tropospheric integrated content of CO_2 covering the range 100-600 hPa (roughly 5-15 km), with the highest sensitivity around 250 hPa in the tropics. The sensitivity to lower atmospheric layers for AIRS than for IASI comes from the use of AIRS channels located at 4.3 μm , which are sensitive to higher pressure than channels located at 15 μm , the only ones used for IASI.



4. Output data

Six Level 2 products derived from combined IASI/AMSU spectral data are delivered by CNRS-LMD:

- CO2_IASA_NLIS: CO₂ from IASI/Metop-A.
- CH4_IASA_NLIS: CH₄ from IASI/Metop-A.
- CO2_IASB_NLIS: CO₂ from IASI/Metop-B.
- CH4_IASB_NLIS: CH₄ from IASI/Metop-B.
- CO2_IASC_NLIS: CO₂ from IASI/Metop-C.
- CH4_IASC_NLIS: CH₄ from IASI/Metop-C.

These products are mid-tropospheric columns retrieved by the CNRS-LMD non-linear inference scheme (NLIS) algorithm, which is discussed in Section 3.

Another product (a brokered product from ESA’s GHG-CCI project) is mid-tropospheric CO₂ from AIRS and the corresponding algorithm is also described in this document.

The retrieval outputs are provided as daily netCDF files. Additional information, such as quality flags, averaging kernels, and geolocation information are also recorded in these files.

Note that the format of the main output data, which are the Level 2 data products, is described in the separate Product User Guide and Specification (PUGS) document. For convenience, we detail the format in the following tables for MT-CH4 (see Table 1) and then MT-CO2 (see Table 2) products.

Table 1: Format of the MT-CH4 product.

Format	
	netCDF4, because compatible to HDF-5 (if not possible CDF3 also allowed) : netcdf=4.7.4,hdf5=1.10.7
Filename	
	daily MT-CH4 IASI-A: CH4_IASIA_NLIS_v<version>_<year><month><day>.nc
	daily MT-CH4 IASI-B: CH4_IASIB_NLIS_v<version>_<year><month><day>.nc
	daily MT-CH4 IASI-C: CH4_IASIC_NLIS_v<version>_<year><month><day>.nc
Global attributes	
	<code>title</code> = "NLIS"
	<code>institution</code> = "Laboratoire de Météorologie Dynamique (LMD) - CNRS"
	<code>source</code> = ""
	<code>history</code> = ""
	<code>reference</code> = "Crevoisier et al., ACP, 2009, 2013"
	<code>tracking_id</code>
	<code>Conventions</code> = "CF-1.6"
	<code>Product_Version</code> = "10.2"



summary = "The non linear inference sheme developed at CNRS-LMD is designed to retrieve mid-tropospheric columns of atmospheric methane (CH4) from radiances measured by the IASI (Infrared Atmospheric Sounding Interferometer) and AMSU (Advanced Microwave Sounding Unit) instruments onboard the Metop platforms. Retrievals are performed for clear-sky situations over land and sea, by day and night, at the spot resolution."
keywords = "satellite, atmosphere, methane"
id = "<filename>"
Naming_authority = "lmd.fr"
keywords_vocabulary = ""
cdm_data_type = "point"
date_created
creator_name = "Cyril Crevoisier"
creator_url = "https://abct.lmd.polytechnique.fr"
creator_email = "cyril.crevoisier@lmd.ipsl.fr"
project = ""
geospatial_lat_min = "-90.f"
geospatial_lat_max = "90.f"
geospatial_lat_units = "degrees_north"
geospatial_lon_min = "-180.f"
geospatial_lon_max = "180.f"
geospatial_lon_units = "degrees_east"
geospatial_vertical_min = " 0.05f"
geospatial_vertical_max = "1013.25f"
time_coverage_start
time_coverage_end
time_coverage_duration = "P1D"
time_coverage_resolution = "P1D"
standard_name_vocabulary = "NetCDF Climate and Forecast (CF) Metadata Conventions Version 1.6"
license = "ESA CCI Data Policy: free and open access"
platform = "Metop-"
sensor = "IASI"
spatial_resolution = ""
Auxiliary variables
latitude (Center latitude of the measurement)
longitude (Center longitude of the measurement)
time (seconds since 1970-1-1 0:0:0)
solar_zenith_angle (Solar zenith angle is the the angle between the line of sight to the sun and the local vertical)
sensor_zenith_angle (Sensor zenith angle is the angle between the line of sight to the sensor and the local vertical)
ch4_quality_flag (quality flag: 0=good, 1=bad)
ch4 (Retrieved mid-tropospheric column of atmospheric methane (CH4) in ppb)
ch4_uncertainty (1-sigma uncertainty of the retrieved MT-CH4 in ppb)
ch4_averaging_kernel (The normalized column-averaging kernel represents the sensitivity of the retrieved MT-CH4 to the atmospheric methane mole fraction depending on pressure (height). All values represent layer averages within the corresponding pressure levels)



pressure_levels (Pressure levels define the boundaries of the averaging kernel. Surface pressure is represented by the 1st element, i.e., profiles are ordered from surface to top of atmosphere)
pressure_weight (Layer dependent weights corresponding to pressure levels)
Obligatory qualifier attributes for each variable
long_name
standard_name (see CF standard name list)
units (unless dimensionless variable: can be missing or then set to "no_units")
valid_range
_FillValue : missing_value (no value provided, agreed to be -999)

Table 2: Format of the MT-CO2 product.

Format
netCDF4, because compatible to HDF-5 (if not possible CDF3 also allowed) : netcdf=4.7.4,hdf5=1.10.7
Filename
daily MT-CO2 IASI-A: CO2_IASIA_NLIS_v<version>_<year><month><day>.nc
daily MT-CO2 IASI-B: CO2_IASIB_NLIS_v<version>_<year><month><day>.nc
daily MT-CO2 IASI-C: CO2_IASIC_NLIS_v<version>_<year><month><day>.nc
Global attributes
iitle = "NLIS"
institution = "Laboratoire de Météorologie Dynamique (LMD) - CNRS"
source = ""
history = ""
reference = "Crevoisier et al., ACP, 2009, 2013"
tracking_id
Conventions = "CF-1.6"
Product_Version = "10.1"
summary = "The non linear inference sheme developed at CNRS-LMD is designed to retrieve mid-tropospheric columns of atmospheric carbon dioxide (CO2) from radiances measured by the IASI (Infrared Atmospheric Sounding Interferometer) and AMSU (Advanced Microwave Sounding Unit) instruments onboard the Metop platforms. Retrievals are performed for clear-sky situations over land and sea, by day and night, at the spot resolution."
keywords = "satellite, atmosphere, carbon dioxide"
id = "<filename>"
Naming_authority = "lmd.fr"
keywords_vocabulary = ""
cdm_data_type = "point"
date_created
creator_name = "Cyril Crevoisier"
creator_url = "https://abct.lmd.polytechnique.fr"
creator_email = "cyril.crevoisier@lmd.ipsl.fr"
project = ""



geospatial_lat_min = "-90.f"
geospatial_lat_max = "90.f"
geospatial_lat_units = "degrees_north"
geospatial_lon_min = "-180.f"
geospatial_lon_max = "180.f"
geospatial_lon_units = "degrees_east"
geospatial_vertical_min = " 0.05f"
geospatial_vertical_max = "1013.25f"
time_coverage_start
time_coverage_end
time_coverage_duration = "P1D"
time_coverage_resolution = "P1D"
standard_name_vocabulary = "NetCDF Climate and Forecast (CF) Metadata Conventions Version 1.6"
license = "ESA CCI Data Policy: free and open access"
platform = "Metop-"
sensor = "IASI"
spatial_resolution = ""
Auxiliary variables
latitude (Center latitude of the measurement)
longitude (Center longitude of the measurement)
time (seconds since 1970-1-1 0:0:0)
solar_zenith_angle (Solar zenith angle is the the angle between the line of sight to the sun and the local vertical)
sensor_zenith_angle (Sensor zenith angle is the angle between the line of sight to the sensor and the local vertical)
co2_quality_flag (quality flag: 0=good, 1=bad)
co2 (Retrieved mid-tropospheric column of atmospheric carbon dioxide (CO2) in ppm)
co2_uncertainty (1-sigma uncertainty of the retrieved MT-CO2 in ppm)
co2_averaging_kernel (The normalized column-averaging kernel represents the sensitivity of the retrieved MT_CO2 to the atmospheric CO2 mole fraction depending on pressure (height). All values represent layer averages within the corresponding pressure levels)
pressure_levels (Pressure levels define the boundaries of the averaging kernel. Surface pressure is represented by the 1st element, i.e., profiles are ordered from surface to top of atmosphere)
pressure_weight (Layer dependent weights corresponding to pressure levels)
Obligatory qualifier attributes for each variable
long_name
standard_name (see CF standard name list)
units (unless dimensionless variable: can be missing or then set to "no_units")
valid_range
_FillValue: missing_value (no value provided, agreed to be -999)



References

- Buchwitz et al., 2015:** Buchwitz, M., Reuter, M., Schneising, O., Boesch, H., Guerlet, S., Dils, B., Aben, I., Armante, R., Bergamaschi, P., Blumenstock, T., Bovensmann, H., Brunner, D., Buchmann, B., Burrows, J.P., Butz, A., Chédin, A., Chevallier, F., Crevoisier, C.D., Deutscher, N.M., Frankenberg, C., Hase, F., Hasekamp, O.P., Heymann, J., Kaminski, T., Laeng, A., Lichtenberg, G., De Mazière, M., Noël, S., Notholt, J., Orphal, J., Popp, C., Parker, R., Scholze, M., Susmann, R., Stiller, G.P., Warneke, T., Zehner, C., Bril, A., Crisp, D., Griffith, D.W.T., Kuze, A., O'Dell, C., Oshchepkov, S., Sherlock, V., Suto, H., Wennberg, P., Wunch, D., Yokota, T., Yoshida, Y., The Greenhouse Gas Climate Change Initiative (GHG-CCI): comparison and quality assessment of near-surface-sensitive satellite-derived CO₂ and CH₄ global data sets. *Remote Sens. Environ.* 162:344–362, <http://dx.doi.org/10.1016/j.rse.2013.04.024>, 2015.
- Chédin et al. 2003:** Chédin, A., Saunders, R., Hollingsworth, A., Scott, N. A., Matricardi, M., Etcheto, J., Clerbaux, C., Armante, R. and Crevoisier, C.: The feasibility of monitoring CO₂ from high resolution infrared sounders. *J. Geophys. Res.*, 108, ACH 6-1–6-19, doi: 10.1029/2001JD001443, 2003.
- Crevoisier et al., 2003:** Crevoisier, C., Chedin, A. and Scott, N.A., AIRS channel selection for CO₂ and other trace-gas retrievals 129, 2719–2740. doi:10.1256/qj.02.180, 2003.
- Crevoisier, 2004:** Crevoisier, C., Etude de la distribution du CO₂ atmosphérique à partir des observations infrarouges à haute résolution spectrale de l'instrument Aqua/AIRS, Thèse de doctorat de l'Université Denis Diderot (Paris VII), 15 octobre 2004.
- Crevoisier et al., 2004:** Crevoisier, C., S. Heilliette, A. Chédin, S. Serrar, R. Armante, and N. A. Scott, Midtropospheric CO₂ concentration retrieval from AIRS observations in the tropics, *Geophys. Res. Lett.*, 31, L17106, doi:10.1029/2004GL020141, 2004.
- Crevoisier et al., 2009a:** Crevoisier, C., Chédin, A., Matsueda, H., et al., First year of upper tropospheric integrated content of CO₂ from IASI hyperspectral infrared observations, *Atmos. Chem. Phys.*, 9, 4797-4810, 2009.
- Crevoisier et al. 2009b:** Crevoisier, C., Nobileau, D., Fiore, A., Armante, R., Chédin, A., and Scott, N. A.: Tropospheric methane in the tropics – first year from IASI hyperspectral infrared observations, *Atmos. Chem. Phys.*, 9, 6337–6350, doi:10.5194/acp-9-6337-2009, 2009b.
- Crevoisier et al., 2013:** Crevoisier, C., Nobileau, D., Armante, R., et al., The 2007–2011 evolution of tropical methane in the mid-troposphere as seen from space by MetOp-A/IASI, *Atmos. Chem. Phys.*, 13, 4279-4289, 2013.
- Crevoisier C., 2018:** Crevoisier C.: Use of Hyperspectral Infrared Radiances to Infer Atmospheric Trace Gases. In S. Liang (Ed.), *Comprehensive Remote Sensing*, vol. 7, pp. 345–387. Oxford: Elsevier, 2018.
- ESA-CCI-GHG-URDv3.0:** Chevallier, F., et al., User Requirements Document (URD), ESA Climate Change Initiative (CCI) GHG-CCI project, Version 3.0, 17 Feb 2020, pp. 42, link: https://www.iup.uni-bremen.de/carbon_ghg/docs/GHG-CCIplus/URD/URDv3.0_GHG-CCIp_Final.pdf, 2020.
- GCOS-154:** Global Climate Observing System (GCOS): SYSTEMATIC OBSERVATION REQUIREMENTS FOR SATELLITE-BASED DATA PRODUCTS FOR CLIMATE - 2011 Update - Supplemental details to the



satellite-based component of the “Implementation Plan for the Global Observing System for Climate in Support of the UNFCCC (2010 Update)”, December 2011, prepared by World Meteorological Organization (WMO), Intergovernmental Oceanographic Commission, United Nations Environment Programme (UNEP), International Council for Science, Doc.: GCOS 154, 2011.

GCOS-200: The Global Observing System for Climate: Implementation Needs, World Meteorological Organization (WMO), GCOS-200 (GOOS-214), pp. 325, link: http://unfccc.int/files/science/workstreams/systematic_observation/application/pdf/gcos_ip_10oct2016.pdf, 2016.

Jacquinet-Husson et al., 2008: Jacquinet-Husson, N., Scott, N. A., Chédin, A., Crépeau, L., Armante, R., Capelle V., and 47 co-authors, The GEISA spectroscopic database: Current and future archive for Earth and planetary atmosphere studies, *J. Quant. Spectrosc. Radiat. Transfer*, 109, 1043–1059, 2008.

Jacquinet-Husson et al., 2011: Jacquinet-Husson, N., Crepeau, L., Armante, R., et al. (2011). The 2009 edition of the GEISA spectroscopic database. *J. Quant. Spectrosc. Radiat. Transf.* 112, 2395–2445. doi:10.1016/j.jqsrt.2011.06.004.

Jason, 2008: Jason, L., README Document for AIRS Level-2 Version 005 Standard Products. In Goddard Earth Sciences Data And Information Services Center (Ed., National Aeronautics and Space Administration (NASA), 2008.

Machida et al. 2008: Machida, T., Matsueda, H., Sawa, Y., Nakagawa, Y., Hirotsu, K., Kondo, N., Goto, K., Nakazawa, T., Ishikawa, K., and Ogawa, T.: Worldwide measurements of atmospheric CO₂ and other trace gas species using commercial airlines, *J. Atmos. Ocean. Tech.*, 25(10), 1744–1754, doi:10.1175/2008JTECHA1082.1, 2008.

Matsueda et al. 2008: Matsueda, H., Machida, T., Sawa, Y., Nakagawa, Y., Hirotsu, K., Ikeda, H., Kondo, N., and Goto, K.: Evaluation of atmospheric CO₂ measurements from new flask air sampling of JAL airliner observation, *Pap. Meteorol. Geophys.*, 59, 1–17, 2008.

Membrive et al. 2016: Membrive, O., Crevoisier, C., Sweeney, C., Danis, F., Hertzog, A., Engel, A., Bönisch, H., and Picon, L.: AirCore-HR: A high resolution column sampling to enhance the vertical description of CH₄ and CO₂, *Atmos. Meas. Tech. Discuss.*, doi:10.5194/amt-2016-236, 2016.

Rumelhart et al., 1986: Rumelhart, D.E. and McClelland, J.L. (1986) University of California, S.D.P.R.G. Parallel distributed processing : explorations in the microstructure of cognition, Parallel distributed processing: explorations in the microstructure of cognition, vol. 1. MIT Press.

Scott, 1974: Scott, N.A., A direct method of computation of the transmission function of an inhomogeneous gaseous medium— I: Description of the method. *J. Quant. Spectrosc. Radiat. Transf.* 14, 691–704. doi:10.1016/0022-4073(74)90116-2, 1974.

Scott and Chédin, 1981: Scott, N.A. and Chédin, A., A Fast Line-by-Line Method for Atmospheric Absorption Computations: The Automatized Atmospheric Absorption Atlas. *J. Appl. Meteorol.* 20, 802–812. doi:10.1175/1520-0450(1981)020<0802:AFLBLM>2.0.CO;2, 1981.

TRD GHG, 2017: Buchwitz, M., Aben, I., Anand, J., Armante, R., Boesch, H., Crevoisier, C., Detmers, R. G., Hasekamp, O. P., Reuter, M., Schneising-Weigel, O., Target Requirement Document, Copernicus Climate Change Service (C3S) project on satellite-derived Essential Climate Variable



(ECV) Greenhouse Gases (CO₂ and CH₄) data products (project C3S_312a_Lot6), Version 1, 28-March-2017, pp. 52, 2017.

Copernicus Climate Change Service

ECMWF - Shinfield Park, Reading RG2 9AX, UK

Contact: <https://support.ecmwf.int/>

climate.copernicus.eu

copernicus.eu

ecmwf.int